Synthesis, characterization, and thermal behavior of palladium(II) complexes containing 4-iodopyrazole

ARTICLE *in* JOURNAL OF THERMAL ANALYSIS AND CALORIMETRY · SEPTEMBER 2014

Impact Factor: 2.04 · DOI: 10.1007/s10973-014-3925-x

J Therm Anal Calorim (2014) 117:1327–1334
DOI 10.1007/s10973-014-3925-x

Synthesis, characterization, and thermal behavior of palladium(II) complexes containing 4-iodopyrazole

Cristiana da Silva · Dênis A. M. da Silva · Fillipe V. Rocha · Carolina V. Barra · Regina C. G. Frem · Adelino V. G. Netto · Antonio E. Mauro · Eduardo T. de Almeida

Received: 8 November 2013 / Accepted: 4 June 2014 / Published online: 20 July 2014

Abstract The mononuclear pyrazolyl complexes $[PdCl_2(HIPz)_2]$ (**1**), $[PdBr_2(HIPz)_2]$ (**2**), $[PdI_2(HIPz)_2]$ (**3**), $[Pd(SCN)_2(HIPz)_2]$ (**4**), and $[Pd(NHCOIPz)_2]$ (**5**) have been prepared. Compound **1** was obtained from the displacement of acetonitrile from $[PdCl_2(CH_3CN)_2]$ precursor by the 4-iodopyrazole (HIPz) ligand, whereas **2**–**5** were synthesized by substitution of the chlorido in **1** by the respective anionic group. The compounds were characterized by elemental analysis, infrared spectroscopy, and ^1H NMR spectroscopy. The thermal behavior of **1**–**5** has been studied by TG and DTA. The thermal stability of $[PdX_2(HIPz)_2]$ compounds varies according to the trends $X = Cl^- < I^- \cong SCN^- < Br^-$. No stable intermediates were isolated during the thermal decompositions due to the overlap of the degradation processes. The final products of the thermal decompositions were characterized as metallic palladium by X-ray powder diffraction.

Keywords Palladium(II) · 4-Iodopyrazole · TG · DTA · IR spectroscopy · NMR spectroscopy

C. da Silva (✉) · D. A. M. da Silva · F. V. Rocha · C. V. Barra · R. C. G. Frem (✉) · A. V. G. Netto · A. E. Mauro
Departamento de Química Geral e Inorgânica, Instituto de Química, UNESP-Univ Estadual Paulista, Araraquara, SP CEP 14801-970, Brazil
e-mail: cristiana_silva28@yahoo.com.br

R. C. G. Frem
e-mail: rcgfrem@iq.unesp.br

E. T. de Almeida
Universidade Federal de Alfenas, Alfenas, MG CEP 31130-000, Brazil

Introduction

Pyrazolyl-based metal compounds have attracted considerable interest from the point of view of their vast structural diversity [1–5] and their potential uses in many different fields, such as catalysis [6], antitumour agents [7, 8], gas storage [9, 10], liquid crystals [11], vapochromic sensors [12], and phosphorescent materials [13]. The versatility in the coordination modes of pyrazoles is based on their amphiprotic behavior, since they possess a Lewis acid pyrrolic N–H group and a Lewis basic pyridinic N-donor [14–16]. In addition, their solubility and donor properties can be fine-tuned by varying the substitution of the 3-, 4-, and 5-position without affecting the environment around the metal.

Particularly, the interest on the thermal behavior of Pd(II) complexes bearing pyrazole-type ligands has been renewed as a number of newly synthesized derivatives turned out to display enhanced thermal stability, compared to complexes bearing many other types of ligands. Many authors have been taking advantage from such property aiming at using these compounds as precursors in atomic layer deposition [17] and chemical vapor deposition, film growth processes [18]. In addition, several studies have demonstrated that the residue formed from thermolysis is dependent on the type of pyrazolyl ligand in the precursor complexes [19, 20]. According to Pérez et al. [20], on heating pyrazolyl Pd(II) complexes to 900 °C in dynamic air atmosphere, the final residue is Pd in purity close to 95 %. Sharma et al. [21] have developed a single-source synthesis of Pd_4Se and PdSe nanoparticles, capped with trioctylphosphine, by thermolysis of palladium(II) complexes containing pyrazolyl-based selenoethers. These findings clearly demonstrate that more systematic studies on the thermal behavior of this class of compounds are

required in order to investigate their potentialities in the above-mentioned fields.

Over the past years, Pd(II) derivatives containing halides and pseudohalides have been one of our research interests [22–27]. In our previous articles [28–31], we described the spectral and thermal studies of a series of palladium(II) complexes of the type $[PdX_2L_2]$ {X = Cl^-, Br^-, I^-, SCN^-; L = pyrazole; 3,5-dimethypyrazole; 4-methylpyrazole; 3,5-dimethyl-4-iodopyrazole, 1-phenyl-3-methylpyrazole}. As a continuation of this systematic work, we present herein the preparation, spectroscopic characterization, and thermal studies on the compounds $[PdCl_2(HIPz)_2]$ (**1**), $[PdBr_2(HIPz)_2]$ (**2**), $[PdI_2(HIPz)_2]$ (**3**), $[Pd(SCN)_2(HIPz)_2]$ (**4**), and $[Pd(NHCOIPz)_2]$ (**5**) {HIPz = 4-iodopyrazole}.

Experimental

General comments

The materials used in the syntheses were all commercially available and were used without purification. All solvents were dried and kept over molecular sieves prior to use. Literature procedures were followed for the synthesis of $[PdCl_2(MeCN)_2]$ [32].

Synthesis of $[PdCl_2(HIPz)_2]$ (**1**)

A solution containing 4-iodopyrazole (157 mg; 0.809 mmol) in 2 mL of ethanol was added to a deep orange solution of $[PdCl_2(MeCN)_2]$ (100 mg; 0.385 mmol) in 15 mL of a mixture $CH_3OH/CHCl_3$ (2:1). The starting orange solution changes to a yellow suspension at the end of the addition. The solid was isolated by filtration, washed with methanol, and dried under vacuum. Yield 75 %. M.p. >248 °C (dec.). *Anal*. Calcd. for $C_6H_6N_4Cl_2I_2Pd$(%): C, 12.75; N, 9.91; H, 1.07. Found: C, 12.39; N, 9.43; H, 1.50.

Synthesis of $[PdBr_2(HIPz)_2]$ (**2**)

A solution containing 4-iodopyrazole (157 mg; 0.809 mmol) in 2 mL of ethanol was added to a deep orange solution of $[PdCl_2(MeCN)_2]$ (100 mg; 0.385 mmol) in 15 mL of a mixture $CH_3OH/CHCl_3$ (2:1), warmed to 60 °C. After stirring the yellow suspension for 5 min, KBr (138 mg; 1.156 mmol) in 2 mL of H_2O was added, affording a deep yellow suspension. The solid was isolated by filtration, washed with methanol, and dried under vacuum. Yield 45 %. M.p. >222 °C (dec.). *Anal*. Calcd. for $C_6H_6N_4Br_2I_2Pd$(%): C, 11.02; N, 8.56; H, 0.92. Found: C, 10.68; N, 8.28; H, 1.05.

Synthesis of $[PdI_2(HIPz)_2]$ (**3**)

To a deep orange solution of $[PdCl_2(MeCN)_2]$ (100 mg; 0.385 mmol) in 15 mL of a mixture $CH_3OH/CHCl_3$ (2:1), it was added 157 mg of 4-iodopyrazole (0.809 mmol) dissolved in 2 mL of ethanol. After stirring the yellow suspension for 5 min, NaI (121 mg; 0.810 mmol) in 2 mL of H_2O was added, and the suspension became red. The solid was isolated by filtration, washed with methanol, and dried under vacuum. Yield 45 %. M.p. >163 °C (dec.). *Anal*. Calcd. for $C_6H_6N_4I_4Pd$(%): C, 9.63; N, 7.49; H, 0.81. Found: C, 9.28; N, 7.14; H, 0.74.

Synthesis of $[Pd(SCN)_2(HIPz)_2]$ (**4**)

A solution containing 4-iodopyrazole (157 mg; 0.809 mmol) in 2 mL of ethanol was added to a deep orange solution of $[PdCl_2(MeCN)_2]$ (100 mg; 0.385 mmol) in 15 mL of a mixture $CH_3OH/CHCl_3$ (2:1). After stirring the yellow suspension for 5 min, NaSCN (66 mg; 0.815 mmol) in 2 mL of H_2O was added, leading to a red solution which was left to evaporate at r.t. After 24 h, an orange precipitate was formed. The solid was isolated by filtration, washed with methanol, and dried under vacuum. Yield 50 %. M.p. >184 °C (dec.). *Anal*. Calcd. for $C_8H_6N_6S_2I_2Pd$(%): C, 15.74; N, 13.76; H, 0.99. Found: C, 16.08; N, 13.57; H, 1.46.

Synthesis of $[Pd(IPzNHCO)_2]$ (**5**)

To a deep orange solution of $[PdCl_2(MeCN)_2]$ (100 mg; 0.385 mmol) in 15 mL of a mixture $CH_3OH/CHCl_3$ (2:1), it was added 157 mg of 4-iodopyrazole (0.809 mmol) dissolved in 2 mL of ethanol. After stirring the yellow suspension for 5 min, KNCO (66 mg; 0.810 mmol) in 2 mL of H_2O was added and the suspension became pale yellow. The solid was isolated by filtration, washed with methanol, and dried under vacuum. Yield 75 %. M.p. >167 °C (dec.). *Anal*. Calcd. for $C_8H_6N_6O_2I_2Pd$(%): C, 16.61; N, 14.53; H, 1.04. Found: C, 16.18; N, 14.20; H, 0.74.

Instrumentation

Elemental analyses of carbon, nitrogen, and hydrogen were performed on a microanalyser CE Instruments, model EA 1110—CHNS-O. Infrared spectra were recorded as KBr pellets on a Nicolet FTIR-Impact 400 spectrophotometer (range 4000–400 cm^{-1}). ^1H NMR spectra were recorded in dmso-d_6 solutions at room temperature on a Brucker AC-200 spectrophotometer working at 200 MHz for hydrogen, using $SiMe_4$ as internal standard. Simultaneous thermal analysis (TG–DTA) was carried out using a TA

Fig. 1 Proposed structures of the complexes **1–5**

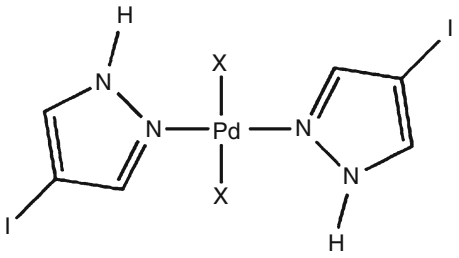

X = Cl (1), Br (2), I (3), SCN (4)

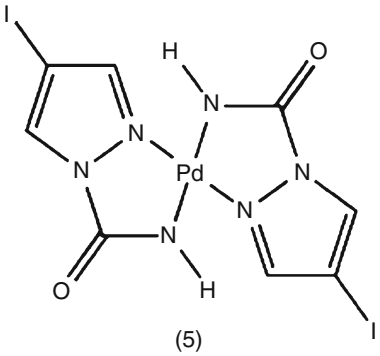

(5)

Table 1 Selected vibrational data/cm^{-1} for complexes **1–5**

Compound					Assignment
1	**2**	**3**	**4**	**5**	
3317 s	3259 s	3254 s	3300–2700 br	3500–3200 br	νNH
3134 m	3109 m	3118 m	–	3124 m	νCH
–	–	–	2118 s		ν_{as}SCN
–	–	–	–	1710 s	νCO
1514 w	1514 *w*	1514 *w*	1529 w	1508 w	Ring breathing
1464 w	1456 w	1456 w	1481 w	1464 w	ν_{ring} + βNH + βCH
1381 m	1383 m	1379 m	1375 m	1380 w	ν_{ring} + β_{ring} + βNH
1344 m	1344 sh	1344 m	1344 sh	1344 m	ν_{ring} + βCH + βNH
1190 w	1186 w	1182 w	1197 w	1169 w	ν_{ring} + βCH + βNH
1124 s	1132 m	1124 s	1138 s	1124 w	ν_{ring} + βCH + βNH
1057 s	1063 s	1055 s	1065 s	1065 m	βCH
941 m	939 mw	939 m	943 s	941 m	β_{ring}
845 m	862 mw	860 m	858 s	825 m	γCH + γNH
675 s	665 s	661 s		648 w	γCH + γNH
577 s	573 s	561 s	599 s	586 w	γ_{ring} + γNH
368 w	377 w	377 w	378 w	378 w	νPdN

Intensities: *s* strong, *m* medium, *w* weak, *sh* shoulder, *ν* stretching, *β* in-plane bending, *γ* out-of-plane bending

Instruments–Q 600, under flow of dry synthetic air (100 mL min^{-1}), temperature up to 900 °C and heating rate of 20 °C min^{-1}, in α-alumina sample holders, using sample masses about 9 mg. The reference substance was pure α-alumina in DTA measurements. X-ray powder patterns of the residues were measured on a Siemens D-5000 X-ray diffractometer using Cu K_α radiation ($\lambda = 1.541$ Å) and setting of 34 kV and 20 mA. The peaks were identified using ICDD bases [33]. Melting/decomposition points were determined on a Mettler FP-2 apparatus.

Results and discussion

The syntheses were carried out at room temperature, with constant magnetic stirring and the complexes obtained were air stable and insoluble in most of organic solvents, except in dmso and dmf. The elemental analysis and thermogravimetric data, together with IR and NMR spectroscopy results, confirmed the proposed formulae for the synthesized compounds, depicted in Fig. 1.

Infrared spectroscopy

The infrared data are summarized in Table 1.

The IR spectrum of the Pd(II) precursor showed the characteristic νCN band of the CH_3CN ligand at 2329 cm^{-1} [32]. Such absorption disappeared in the IR spectra of **1–5**, indicating the displacement of acetonitrile by 4-iodopyrazole ligand. Except in **5**, the monodentate neutral coordination of the pyrazolyl ligand was evidenced by the appearance of strong νNH bands around 3300 cm^{-1}

Table 2 ^{1}H chemical shifts/ppm for compounds **1–4**

Numbering scheme I		^{1}H NMR data		
		NH	H_3	H_5
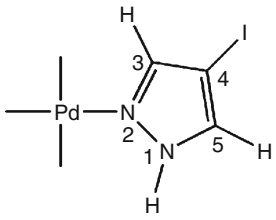	HIPZ	13.16	7.86	7.56
	1	13.76	8.11	7.74
	2	[a]	8.12	7.81
	3	14.31	8.28	8.15
	4	14.46	7.66	7.32

For labeling pyrazolate protons, see Scheme I. Coupling constants could not be determined due to the broadening of signals

[a] not observed

and by shift of the band attributed to the ring breathing mode to lower frequency (ca. 1514 cm^{-1}) when compared with that one of the free ligand (1,534 cm^{-1}) [34–36]. The displacement of the chlorido from $[PdCl_2(CH_3CN)_2]$ precursor by thiocyanato ligand was proved by the presence of a new, strong band at 2118 cm^{-1} and another weak absorption at 427 cm^{-1} observed in the IR spectrum of **4**, assigned to ν_{as}SCN and δNCS modes, respectively, which are consistent with terminal *S*-bonded thiocyanate [37–40]. The formation of the 1-carbamoyl-4-iodopyrazole ligand in the chelate **5** via 1,3-dipolar cycloaddition reaction between the Pd(pyrazolyl ligand) moiety and NCO group, was evidenced by the existence of a strong νCO band located at 1710 cm^{-1} [29–31]. Further evidence of the formation of the chelated addition product **5** was given by the absence of the usual ν_{as}NCO absorption in the 2250–2200 cm^{-1} range, typical of terminally coordinated NCO group [39, 40].

Far IR spectra

In the far IR spectra of **1–5**, the coordination of the pyrazolyl ligand was also verified by the existence of a νPd–N(pyrazole) band in the spectral range of 378–368 cm^{-1}. It is worth mentioning that such absorption is absent in the spectrum of free HIPz. Besides that, the far IR spectra of halogeno-complexes $[PdX_2(HIPz)_2]$, {X = Cl^-(**1**), Br^-(**2**), I^-(**3**)}, showed one νPd–X absorption at 287 (**1**), 230 (**2**), and 204 cm^{-1} (**3**), as expected for complexes possessing the *trans* configuration (D_{2h}) [37, 41].

^{1}H NMR spectra

The ^{1}H NMR data are given in Table 2. Coupling constants could not be determined due to the broadening of signals. Compound **5** was not soluble enough to allow solutions suitable for NMR analysis.

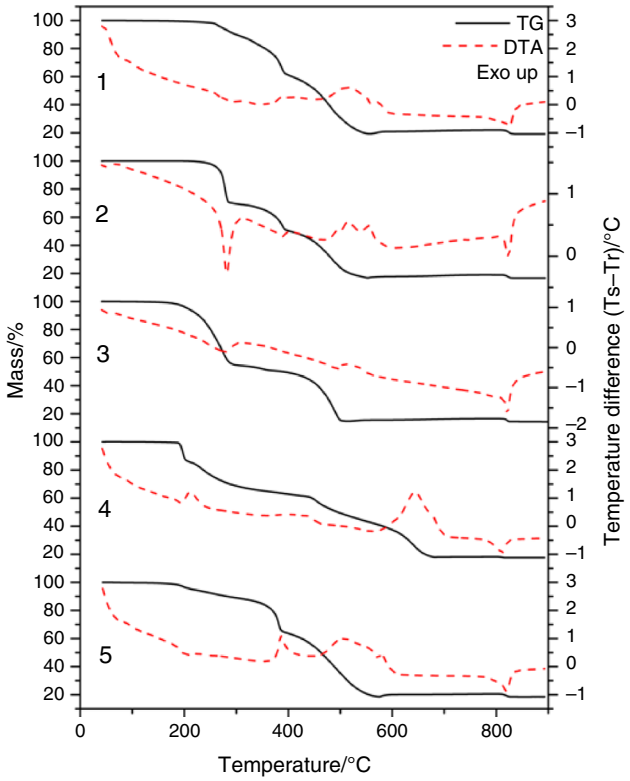

Fig. 2 TG and DTA curves of the compounds: $[PdCl_2(HIPz)_2]$ (**1**), m_i = 9.3953 mg; $[PdBr_2(HIPz)_2]$ (**2**), m_i = 8.93283 mg; $[PdI_2(HIPz)_2]$ (**3**), m_i = 9.48098 mg; $[Pd(SCN)_2(HIPz)_2]$ (**4**), m_i = 9.06308 mg; $[Pd(IPzNHCO)_2]$ (**5**), m_i = 9.4499 mg. Heating rate = 20 °C min^{-1}; dry synthetic air atmosphere

The ^{1}H NMR spectrum of the free ligand clearly indicated that the proton exchange in 4-iodopyrazole is slow on the NMR time scale at room temperature due to the appearance of separated H_3 and H_5 signals. The overall pattern of the ^{1}H NMR spectra of the complexes is very similar to that of the free ligand. However, all the signals were shifted upon coordination. The monodentate coordination mode of 4-iodopyrazole in **1–4** was verified by the presence of a low field signal at 14.46–13.76 ppm (NH) and two H_3 and H_5 peaks located in the spectral range 8.28–7.32 ppm (see numbering in Scheme I in Table 2). Interestingly, the ^{1}H NMR spectra obtained from freshly solutions of **1**, **2**, and **3** showed a signal at 7.74 ppm, typical of the free 4-iodopyrazolate ion. Over a period of days, its intensity increases with simultaneous decreasing in intensity of the H_3 and H_5 resonances belonging to the initial complexes in solution. These structural changes in solution might be associated with the steric influence of the bulky halides, since they are more intense in **2** and **3**.

Thermoanalytical studies

The TG and DTA curves for the compounds $[PdCl_2(HIPz)_2]$ (**1**), $[PdBr_2(HIPz)_2]$ (**2**), $[PdI_2(HIPz)_2]$ (**3**),

Table 3 Thermal analysis data for compounds **1**–**5**

Complex	Step	ΔT/°C	Δm/%	DTA peaks/°C	
				Endo	Exo
1	1	124–387	−35.3	288	385
	2	387–554	−45.3	–	512
	3	554–801	+2.7	–	568
	4	801–843	−2.9	809, 823	–
	Residue		19.2		
2	1	205–289	−29.6	282	–
	2	289–397	−19.5	388	497, 515, 556
	3	397–552	−34.1	–	–
	4	552–802	+2.2	823	–
	5	802–836	−2.3		
	Residue		16.6		
3	1	142–288	−43.6	279	–
	2	288–515	−41.8	–	508, 528
	3	515–804	+1.9	–	–
	4	804–851	−2.2	821	–
	Residue		14.4		
4	1	148–203	−14.5	195	211
	2	203–439	−27.6	–	359–457
	3	439–683	−42.9	–	643
	4	683–799	+0.2	–	–
	5	799–823	−0.7	811	–
	Residue		17.5		
5	1	133–347	−14.7	203	–
	2	347–393	−20.7		387
		393–575	−46.0	–	442–616
	2	575–799	+2.0	820	–
	3	799–834	−2.1		–
	Residue		18.5		

$[Pd(SCN)_2(HIPz)_2]$ (**4**), and $[Pd(IPzNHCO)_2]$ (**5**) are shown in Fig. 2. Table 3 lists the initial and final temperatures (°C), partial mass losses (%), and DTA peaks of the thermal studies on compounds **1**–**5**. The final residues were characterized by X-ray powder diffraction, and the peaks were identified using ICDD bases for Pd^0 (card 05-0681) [33]. It is important to emphasize that our propositions have been only based on mass loss calculation from TG curves taking into account the elimination of a given ligand/fragment from the molecular structure of the complexes. It does not mean, however, that these groups have been eliminated in this form.

The TG curve showed that **1** is thermally stable up to 124 °C (Fig. 2). Afterward, the release of the ligands takes place in two steps. The first stage (124–387 °C) is characterized by 35.3 % of mass loss which can be assigned by mass calculation to the elimination of one HIPz ligand (Calcd. 34.3 %). This step is associated with a broad endothermic signal over the temperature range 250–381 °C. The mass loss of 45.3 % between 387 and 554 °C is related to the pyrolysis of the remaining ligands by the presence of an exothermic signal at 512 °C, affording Pd^0 as product. A slight and progressive mass gain of 2.7 % occurred up to 801 °C which is ascribed to the burning of remaining carbonaceous material (exothermic signal at 568 °C) with further conversion of Pd^0 to PdO. The decomposition of PdO to Pd^0 (Calcd. 18.9 %, Found 19.2 %) is observed in the last mass loss (2.9 %) between 801 and 843 °C, which is accompanied by endothermic peaks at 809 and 823 °C.

The TG–DTA curves for compound **2** (Fig. 2) indicated that the first step (205–289 °C) is accompanied by 29.6 % mass loss attributed, by mass calculation, to the release of one HIPz ligand (Calcd. 29.6 %) which is associated with a sharp and intense endothermic signal at 282 °C. A further heating to 397 °C resulted in amass loss of 19.5 % which agrees well with the elimination of one iodine atom from the remaining HIPz ligand (Calcd. 19.5 %). This event is also accompanied by an endothermic peak at 388 °C. The following stage in the process of decomposition (up to 552 °C, $\Delta m = 34.1$ %) consists of the combustion of the remaining organic material due to the appearance of exothermic peaks at 497, 515, and 556 °C in the DTA curve, leading to the formation of Pd^0 as product (Calcd.16.3 %, Found 16.7 %). The third step (552–802 °C) corresponds to the uptake of O_2 and conversion of the Pd^0 to PdO. The last mass loss is characterized by the decomposition of PdO to Pd^0 at 836 °C, which is accompanied by endothermic peaks at 823 °C in the DTA curve.

With regard to the thermal behavior of **3** (Fig. 2), the first stage (142–288 °C) may be assigned, by mass calculation, to the simultaneous elimination of one pyrazolyl ligand and one iodine (Calcd. 42.9 %, found 43.6 %). This process is accompanied by an endothermic signal at 279 °C. A further increasing in temperature up to 515 °C resulted in the total oxidation of the remaining organic material (exothermic peaks at 508 and 528 °C), affording Pd^0 as residue. In the range of 515–804 °C, the mass gain of 1.9 % corresponds to the uptake of oxygen required for oxidation of Pd^0 to PdO. Over the 804–851 °C range, the expected reduction of PdO in Pd^0 (Calcd. 14.3 %, Found 14.4 %) accompanied by the endothermic peak at 821 °C is observed.

According to TG–DTA curves (Fig. 2), the thermal degradation of $[Pd(SCN)_2(HIPz)_2]$ (**4**) takes a different course. Compound **4** is thermally stable up to 148 °C, then undergoes a melting (DTA peak at 195 °C) which is

immediately followed by a small mass loss of 14.5 % accompanied by an exothermic signal at 211 °C. According to mass calculations, this event may be attributed to a partial release of 1.5 SCN (Calcd. 14.3 %). Afterwards, two mass losses over the temperature range of 203–683 °C, are caused by the gradually oxidative degradation of the remaining organic residues, yielding Pd^0 as product. The partial oxidation of Pd^0 is evidenced by a progressive mass in the range of 683–799 °C. The PdO further decomposed into Pd^0 (Calcd. 17.5 %, Found 17.5 %) in the last mass loss, this process is accompanied by an endothermic peak at 811 °C.

TG and DTA curves indicated that complex $[Pd(IPzNHCO)_2]$ (**5**) decomposed into Pd^0 by three consecutive mass changes (Fig. 2). The first step (133–347 °C) is characterized by a mass loss of 14.7 % associated with an endothermic peak at 203 °C which can be assigned by mass calculation to the elimination of two HNCO groups (Calcd. 14.9 %). The next stage of thermal decomposition corresponds to two overlapped mass loss events: an abrupt mass loss of 20.7 % (347–393 °C) accompanied by an exothermic peak at 387 °C, followed by a mass loss of 46.0 % (393–575 °C) associated with a broad exothermic envelop over the temperature range 442–616 °C. These processes are related to the pyrolysis of the remaining ligands, giving rise to Pd^0 as final product (Calcd.18.4 %, Found 18.5 %).

The thermal analysis results (Table 3) indicated that compounds **1** and **2** display a similar decomposition pattern in which the first step is characterized by the release of one HIPz ligand. For complex **3**, our mass calculations indicated that the first mass loss stage coincides with the elimination of one HIPz and one iodide ligands. This finding may suggest that the steric hindrance around the metal environment plays an important role in the mechanism of thermal decomposition. On the other hand, the replacement of two halido by two thiocyanato ligands (**4**) results in a distinct thermal behavior pattern. Even though the interaction between Pd(II) and *S*-thiocyanate groups is favorable from the HSAB principle [42], the polynuclear structure of the pseudohalide may also increase the steric repulsion at metal coordination environment, affecting the thermal stability of the compound.

From the comparison of TG curves of **1** and **4** with their analogous $[PdX_2L_2]$ {L = pyrazole (HPz); 3,5-dimethylpyrazole (HdmPz), 4-methylpyrazole(HmPz), 3,5-dimethyl-4-iodopyrazole (HdmIPz); X = Cl, SCN} [29–31], some interesting trends can be observed. The thermal stability of the compounds $[PdCl_2L_2]$ varies in the sequence:

HdmIPz > HdmPz ≅ HmPz > HPz > HIPz

This finding may indicate that the basicity of the neutral ligands plays an important role in their thermal stability. According to Reedijk et al. [43], the pK_b can be used as a measure for the strength of the interaction between the neutral pyrazolyl ligand and the metal ion complexes. For a particular type of ligand higher basicity or pK_b, which reflects a donor ability toward the "hard acid" H^+, also renders a ligand a better donor toward a "soft acid" [44]. The 4-iodopyrazole (HIPz) displays the lowest pK_b (0.82) among the pyrazoles used in this work: HPz (2.52), HmPz (3.09), HdmPz (4.12), and HdmIPz (2.36) [45]. It seems plausible that the thermal decomposition of $[PdCl_2(HIPz)_2)]$ (**1**) starts a lower temperature than their analogs due to the weaker coordination of HIPz in **1**.

Chelated-complexes comprising 1-carbamoylpyrazole-type ligands display the following thermal stability [29–31]:

IPzNHCO ≅ PzNHCO > dmPzNHCO

TG data showed that the introduction of substituents at the 4 position on the pyrazolyl moiety does not affect significantly the thermal stability of the complexes. While the compounds bearing the unsubstituted and 4-substituted pyrazoles (i.e., $[Pd(PzNHCO)_2]$ and $[Pd(IPzNHCO)_2]$) [29] are stable upto 129 and 133 °C, respectively, the compound $[Pd(dmPzNHCO)_2]$ started to decompose at a temperature lower than the other species, probably due to the steric hindrance introduced by methyl groups at 3 and 5 positions, adjacent to the coordination sites of the pyrazolyl ring [46].

Conclusions

This study describes the synthesis, spectroscopic characterization, and thermal studies of the new palladium(II) complexes bearing 4-iodopyrazole. The IR and ^1H NMR experiments indicated the neutral monodentate coordination of 4-iodopyrazole via pyridine-type nitrogen atom in the **1–4** complexes and the bidentate coordination of the 1-carbamoyl-4-iodopyrazole in **5**.

The thermogravimetric data showed that all decompositions initiate with the release of the ligands in 2 or 3 stages, leading to the formation of Pd^0. The chelated compound $[Pd(IPzNHCO)_2]$ (**5**) exhibited a similar initial decomposition temperature to that of observed for unsubstituted pyrazolyl analog, suggesting that the nature of the substituent at the 4 position on the pyrazolyl moiety does not influence the thermal stability.

Acknowledgements This research was supported by CNPq, FAPESP, Capes, FAPEMIG and FINEP.

References

1. Titov AA, Filippov OA, Bilyachenko AN, Smol'yakov AF, Dolgushin FM, Belsky VK, Godovikov IA, Epstein LM, Shubina ES. Complexes of trinuclear macrocyclic copper(I) and silver(I) 3,5-bis(trifluoromethyl)pyrazolates with ketones. Eur J Inorg Chem. 2012;2012:5554–61.
2. Pérez J, Riera L. Pyrazole complexes and supramolecular chemistry. Eur J Inorg Chem. 2009;2009:4913–25.
3. Halcrow MA. Pyrazoles and pyrazolides-flexible synthons in self-assembly. Dalton Trans. 2009;12:2059–73.
4. Netto AVG, Frem RCG, Mauro AE. A química supramolecular de complexos pirazólicos. Quím Nova. 2008;31:1208–17.
5. Brandi-Blanco P, Miguel PJS, Lippert B. Expected and unconventional Ag^+ binding modes in heteronuclear Pt, Ag coordination polymers derived from *trans*-$[Pt(methylamine)_2(pyrazole)_2]^{2+}$. Eur J Inorg Chem. 2012;2012:1122–9.
6. Albertin G, Antoniutti S, Paganelli S. Trichlorostannyl complexes of iridium with both P-donor and N-donor ligands: preparation and activity as hydrogenation catalysts. J Organomet Chem. 2009;694:3142–8.
7. Rocha FV, Barra CV, Netto AVG, Mauro AE, Carlos IZ, Frem RCG, Ananias SR, Quilles MB, Stevanato A, da Rocha MC. 3,5-Dimethyl-1-thiocarbamoylpyrazole and its Pd(II) complexes: synthesis, spectral studies and antitumor activity. Eur J Med Chem. 2010;45:1698–702.
8. Barra CV, Rocha FV, Gautier A, Morel L, Quilles MB, Carlos IZ, Treu-Filho O, Frem RCG, Mauro AE, Netto AVG. Synthesis, cytotoxic activity and DNA interaction of Pd(II) complexes bearing *N*'-methyl-3,5-dimethyl-1-thiocarbamoylpyrazole. Polyhedron. 2013;65:214–20.
9. Mathivathanan L, Torres-King J, Primera-Pedrozo JN, García-Ricard OJ, Hernández-Maldonado AJ, Santana JA, Raptis RG. Selective CO_2adsorption on metal–organic frameworks based ontrinuclear Cu_3pyrazolatocomplexes: an experimental and computational study. Cryst Growth Des. 2013;13:2628–35.
10. Montoro C, Linares F, Procopio EQ, Senkovska I, Kaskel S, Galli S, Masciocchi N, Barea E, Navarro JAR. Capture of nerve agents and mustard gas analogues by hydrophobic robust MOF-5 type metal-organic frameworks. J Am Chem Soc. 2011;133:11888–91.
11. Barberá J, Lantero I, Moyano S, Serrano JL, Elduque A, Giménez R. Silver pyrazolates as coordination-polymer luminescent metallomesogens. Chem Eur J. 2010;16:14545–53.
12. Rawashdeh-Omary MA, Rashdan MD, Dharanipathi S, Elbjeirami O, Ramesh P, Dias HVR. On/off luminescence vapochromic selective sensing of benzene and its methylated derivatives by a trinuclear silver(I) pyrazolate sensor. Chem Commun. 2011;47:1160–2.
13. Ma B, Djurovich PI, Garon S, Alleyne B, Thompson ME. Platinum binuclear complexes as phosphorescent dopants for monochromatic and white organic light-emitting diodes. Adv Funct Mater. 2006;16:2438–46.
14. Viciano-Chumillas M, Tanase S, de Jongh LJ, Reedijk J. Coordination versatility of pyrazole-based ligands towards high-nuclearity transition-metal and rare-earth clusters. Eur J Inorg Chem. 2010;2010:3403–18.
15. Netto AVG, Frem RCG, Mauro AE. Low-weight coordination polymers derived from the self-assembly reactions of Pd(II) pyrazolyl compounds and azide ion. Polyhedron. 2005;24:1086–92.
16. Da Silva PB, Frem RCG, Netto AVG, Mauro AE, Ferreira JG, Santos RHA. Pyrazolyl coordination polymers of cadmium(II). Inorg Chem Commun. 2006;9:235–8.
17. El-Kaderi OM, Heeg MJ, Winter CH. Tetramethylcyclobuta dienecobalt(I) complexes containing pyrazolate or tetrazolate ligands with various coordination modes. Organomet Chem. 2011;696:1975–81.
18. Chi Y, Lay E, Chou T-Y, Song Y-H, Carty AJ. Deposition of silver thin films using the pyrazolate complex $[Ag(3,5\text{-}(CF_3)_2\text{-}C_3NH_2)]_3$. Chem Vap Depos. 2005;11:206–12.
19. Díaz-Ayala R, Arroyo-Ramírez L, Raptis RG, Cabrera CR. Thermal and surface analysis of palladium pyrazolates molecular precursors. J Therm Anal Calorim. 2014;115:479–88.
20. Pérez J, Serrano JL, Granados JE, Alcolea LA. Recovering palladium from its surplus complexes in research laboratories by solid state thermal treatment. RSC Adv. 2013;3:4558–67.
21. Sharma KN, Joshi H, Singh VV, Singh P, Singh AK. Palladium(II) complexes of pyrazolated thio/selenoethers: syntheses, structures, single source precursors of Pd_4Se and PdSe nanoparticles and potential for catalyzing Suzuki–Miyaura coupling. Dalton Trans. 2013;42:3908–18.
22. Rocha FV, Barra CV, Mauro AE, Carlos IZ, Nauton L, ElGhozzi M, Gautier A, Morel L, Netto AVG. Synthesis, characterization, X-ray structure, DNA cleavage, and cytotoxic activities of palladium(II) complexes of 4-phenyl-3-thiosemicarbazide and triphenylphosphane. Eur J Inorg Chem. 2013;2013:4499–505.
23. Moro AC, Urbaczek AC, de Almeida ET, Pavan FR, Leite CQF, Netto AVG, Mauro AE. Binuclear cyclopalladated compounds with antitubercular activity: synthesis and characterization of $[\{Pd(C^2,N\text{-dmba})(X)\}_2(\mu\text{-bpp})]$ (X = Cl, Br, NCO, N_3; bpp = 1,3-bis(4-pyridyl)propane). J Coord Chem. 2012;65:1434–42.
24. De Almeida ET, Mauro AE, Santana AM, Ananias SR, Netto AVG, Ferreira JG, Santos RHA. Self-assembly of organometallic Pd(II) complexes via $CH_3\cdots\pi$ interactions: the first example of a cyclopalladated compound with herringbone stacking pattern. Inorg Chem Commun. 2007;10:1394–8.
25. Santana AM, Ferreira JG, Moro AC, Lemos SC, Mauro AE, Netto AVG, Frem RCG, Santos RHA. Self-assembly of cyclometallated Pd(II) compounds directed by C–H π interactions: a structural evidence for metalloaromaticity in a cyclopalladated ring. Inorg Chem Commun. 2011;14:83–6.
26. Santana AM, Mauro AE, De Almeida ET, Netto AVG, Klein SI, Santos RHA, Zoia JR. 1,3-dipolar cycloaddition of CS_2 to the coordinated azide in the cyclopalladated $[Pd(bzan)(\mu\text{-}N_3)]_2$. Crystal and molecular structure of di(μ-*N*, *S*-1,2,3,4-thiatriazole-5-thiolate)bis[(benzylideneaniline-C^2, N)palladium(II)]. J Coord Chem. 2001;53:163–72.
27. Mauro AE, Caires ACF, Santos RHA, Gambardella MTD. Cycloaddition reaction of the azido-bridged cyclometallated complex $[Pd(dmba)(\mu\text{-}N_3)]_2$ with CS_2. Crystal and molecular structure of di(μ-*N*,*S*-1,2,3,4-thiatriazole-5-thiolate)bis[(*N*, *N*-dimethylbenzylamine-C^2, N)palladium(II)]. J Coord Chem. 1999;48:521–8.
28. Netto AVG, Takahashi PM, Frem RCG, Mauro AE. Zorel Júnior HE. Thermal decomposition of palladium(II) pyrazolyl complexes, part I. J Anal Appl Pyrolysis. 2004;72:183–9.
29. Netto AVG, Santana AM, Mauro AE, Frem RCG, de Almeida ET, Crespi MS, Zorel HE Jr. Thermal decomposition of palladium(II) pyrazolyl complexes, part II. J Therm Anal Calorim. 2005;79:339–42.
30. Barra CV, Rocha FV, Netto AVG, Shimura B, Frem RCG, Mauro AE, Carlos IZ, Ananias SR, Quilles MB. New palladium(II) complexes with pyrazole ligands: synthesis, spectral and thermal studies and antitumor evaluation, part I. J Therm Anal Calorim. 2011;106:483–8.
31. Barra CV, Rocha FV, Netto AVG, Frem RCG, Mauro AE, Carlos IZ, Ananias SR, Quilles MB. New palladium(II) complexes with pyrazole ligands: synthesis, spectral and thermal studies and antitumor evaluation, part II. J Therm Anal Calorim. 2011;106:489–94.
32. Bego AM, Frem RCG, Netto AVG, Mauro AE, Ananias SR, Carlos IZ, Rocha MC. Immunomodulatory effects of palladium(II) complexes of 1,2,4-triazole on murine peritoneal macrophages. J Braz Chem Soc. 2009;20:437–44.

33. Powder Diffraction File of the Joint Committee on Powder Diffraction Standards. Sets 1–32, published by the International Center of Diffraction Data, Swarthmore, PA 19081, USA (1982).
34. Takahashi PM, Frem RCG, Netto AVG, Mauro AE, Matos JR. Thermal studies on nickel(II) 4-iodoprazole complexes. J Therm Anal Calorim. 2007;87:797–800.
35. Takahashi PM, Netto AVG, Mauro AE, Frem RCG. Thermal study of nickel(II) pyrazolyl complexes. J Therm Anal Calorim. 2005;79:335–8.
36. Da Silva PB, Terra PH, Frem RCG, Netto AVG, Mauro AE. Synthesis, characterization, and investigation of the thermal behavior of Cu(II) pyrazolyl complexes. J Therm Anal Calorim. 2011;106:495–9.
37. Nakamoto K. Infrared and Raman spectra for inorganic and coordination compounds. Part B: applications in coordination, organometallic, and bioinorganic chemistry. 5th ed. New York: A Wiley-Interscience Publication; 1997.
38. Netto AVG, Frem RCG, Mauro AE, Santos RHA, Zoia JR. Crystallographic and spectroscopic studies on palladium(II) complexes containing pyrazole and thiocyanate ligands. Transit Metal Chem. 2002;27:279–83.
39. De Almeida ET, Santana AM, Netto AVG, Torres C, Mauro AE. Thermal study of cyclopalladated complexes of the type $[Pd_2(dmba)_2X_2(bpe)]$—(X = NO_3^-, Cl^-, N_3^-, NCO^-, NCS^-; bpe = trans-1,2-bis(4-pyridyl)ethylene). J Therm Anal Calorim. 2005;82:361–4.
40. de Souza RA, Stevanato A, Treu-Filho O, Netto AVG, Mauro AE, Castellano EE, Carlos IZ, Pavan FR, Leite CQF. Antimycobacterial and antitumor activities of palladium(II) complexes containing isonicotinamide (isn): X-ray structure of *trans*-$[Pd(N_3)_2(isn)_2]$. Eur J Med Chem. 2010;45:4863–8.
41. Van Kralingen CG, de Ridder JK, Reedijk J. Coordination compounds of platinum(II) and palladium(II) with pyrazole as a ligand. New synthetic procedures and characterization. Transit Metal Chem. 1980;5:73–7.
42. Pearson RG. Hard and soft acids and bases. J Am Chem Soc. 1963;85:3533–9.
43. Reedijk J, Windhorst JCA, Van Ham NHM, Groeneveld WL. Pyrazoles and imidazoles as ligands, part IX: some adducts formed between Cu(II) salts and substituted pyrazoles. Rec Trav Chim. 1971;90:234–51.
44. Johnson CR, Henderson WW, Shepherd RE. Pyrazole/imidazole and pyrazolato/imidazolato complexes of pentacyanoferrate(II/III) and pentaammineruthenium(II/III). LMCT transitions of low-Spin d^5 complexes. Inorg Chem. 1984;23:2154–63.
45. Schofield K, Grimmett MR, Keene BRT. "Heteroaromatic nitrogen compounds: the azoles". Cambridge: Cambridge Academic Press; 1976. p. 446.
46. Netto AVG, Frem RCG, Mauro AE, Crespi MS, Zorel HE Jr. Synthesis, spectral, and thermal studies on pyrazolate-bridged palladium(II) coordination polymers. J Therm Anal Calorim. 2007;87:789–92.